Review

Advances in Mechanical Engineering

Advances in Mechanical Engineering
2016, Vol. 8(8) 1–21
© The Author(s) 2016
DOI: 10.1177/1687814016664660
aime.sagepub.com
SAGE

A review of physics-based models in prognostics: Application to gears and bearings of rotating machinery

Adrian Cubillo, Suresh Perinpanayagam and Manuel Esperon-Miguez

Abstract

Health condition monitoring for rotating machinery has been developed for many years due to its potential to reduce the cost of the maintenance operations and increase availability. Covering aspects include sensors, signal processing, health assessment and decision-making. This article focuses on prognostics based on physics-based models. While the majority of the research in health condition monitoring focuses on data-driven techniques, physics-based techniques are particularly important if accuracy is a critical factor and testing is restricted. Moreover, the benefits of both approaches can be combined when data-driven and physics-based techniques are integrated. This article reviews the concept of physics-based models for prognostics. An overview of common failure modes of rotating machinery is provided along with the most relevant degradation mechanisms. The models available to represent these degradation mechanisms and their application for prognostics are discussed. Models that have not been applied to health condition monitoring, for example, wear due to metal–metal contact in hydrodynamic bearings, are also included due to its potential for health condition monitoring. The main contribution of this article is the identification of potential physics-based models for prognostics in rotating machinery.

Keywords

Bearings, condition monitoring, creep, damage mechanics, failure, fracture mechanics, gears, modelling, rotating machinery

Date received: 11 February 2016; accepted: 26 July 2016

Academic Editor: Michal Kuciej

Introduction

Prognostics and Health Management (PHM) refers to the capability to assess the current (diagnostics) and future (prognostics) health state of a system, which can be a machine, a process or a vehicle. As a result, the maintenance plan can be optimized depending on the current health status of the system called predictive maintenance or condition-based maintenance (CBM), instead of relying on historical data and life estimation calculations (preventive maintenance) or reacting only when a failure occurs (reactive maintenance).[1]

The main benefits of a CBM strategy are the time and cost reduction due to the higher efficiency of planned maintenance and the optimization of the component life compared to preventive strategies.[2] However, these benefits must overcome the additional cost of the technology required to implement CBM. Additional benefits include the reduced mean maintenance time due to fault localization, the reduced disruption and the increased safety due to the reduction of unexpected failures.[3,4]

IVHM Centre, Cranfield University, Cranfield, UK

Corresponding author:
Adrian Cubillo, IVHM Centre, Cranfield University, Cranfield MK43 0AL, Bedfordshire, UK.
Email: a.cubillo@cranfield.ac.uk

Creative Commons CC-BY: This article is distributed under the terms of the Creative Commons Attribution 3.0 License (http://www.creativecommons.org/licenses/by/3.0/) which permits any use, reproduction and distribution of the work without further permission provided the original work is attributed as specified on the SAGE and Open Access pages (https://us.sagepub.com/en-us/nam/open-access-at-sage).

Downloaded from ade.sagepub.com at Cranfield University on September 22, 2016

The information generated by a PHM system can be divided into diagnostics and prognostics: diagnostics includes anomaly detection, fault isolation, fault classification and its uncertainty;[5] while prognostics include the estimation of the remaining useful life (RUL), the uncertainty of the prediction and incipient fault detection. Also diagnostics and prognostics knowledge can be used for future improvements of the design.[6,7]

In order to evaluate the health of a system, the various techniques are commonly categorized into data-driven models (DDMs), physics-based models (PbMs) and hybrid models.[8–10] DDMs are based on statistical- and machine-learning techniques and do not rely on the knowledge of the physics that govern the system or its degradation mechanisms:[9] these techniques have proven successful for fault detection,[11] classification[12] and RUL estimation.[13] PbMs consist in the use of mathematical models that describe the physics of the component to assess its current and future health. The performance of PbMs depends on the capability of the models to accurately represent the failure and degradation phenomena. Hybrid models refer to the integration of different models, either using various approaches depending on the task, for instance a DDM for diagnostics and a PbM for prognostics,[14–18] or a combination of several models that represent the same phenomena to obtain a more robust health assessment, so-called ensemble models.[19,20]

The main advantages of machine-learning techniques are their potential to be used in several systems as knowledge of the physics of the system is not required, thus being easily scalable to different systems. However, there are problems such as risk of over fitting[16] and the necessity of large training data sets compared to PbM approaches.[9] Additionally, the synergies between PbMs and models used during the design phase make them particularly suitable when the health condition monitoring system is being developed during the design phase.[10] However, PbMs are not easily scalable because they are system specific and it can be challenging to obtain measurable indicators directly related to the outputs of the PbM.[5]

Reviews covering the state of the art of health condition monitoring for rotating machinery have already been published focusing on the methodologies and algorithms of PHM in rotating equipment,[9,21] and specific techniques such as the empirical mode decomposition for fault diagnosis[22] and vibration analysis.[23] However, the state of the art of PbM for rotating machinery has not been reviewed in depth; papers focused on PHM for rotating machinery normally include a section mentioning significant PbM approaches, but the description of the principles behind those models is limited. This article describes the principles behind the most relevant PbM for rotating machinery and the factors that have to be taken into account when selecting a model for PHM are discussed.

The aim of this article is to review the state of the art of prognostics for rotating machinery based on PbMs. The most important failure modes and the models available to represent their degradation mechanisms are identified, including not only the models already applied on PHM for rotating machinery, but also models that can potentially be used in the future. The concept of PbM and a brief review of parameter estimators are presented in the PbM approach section. Failure modes of rotating machinery section include common failure modes of rotating machinery and examples of PHM solutions for them. The well-accepted models of degradation mechanisms of rotating machinery are described in the relevant degradation models section. Finally, the section 'Conclusion' summarizes the findings of the article and discusses the challenges of applying PbMs for diagnostics and prognostics of rotating machinery.

PbM approach

PbM approaches, also referred to as model-based approaches, assess the health of the system by solving a set of equations derived from engineering and science knowledge,[5] either for diagnostics or for prognostics. However, the main advantage of PbMs consists of using degradation models to predict long-term behaviour.[24] A generic process to develop prognostics based on PbMs that consider a set of equations that define the dynamics and the degradation of the system was proposed by Luo et al.[25] and is shown in Figure 1. It consists of a model of the system and its degradation, where fast dynamic variables represent the behaviour of the system, and slow dynamic variables determine

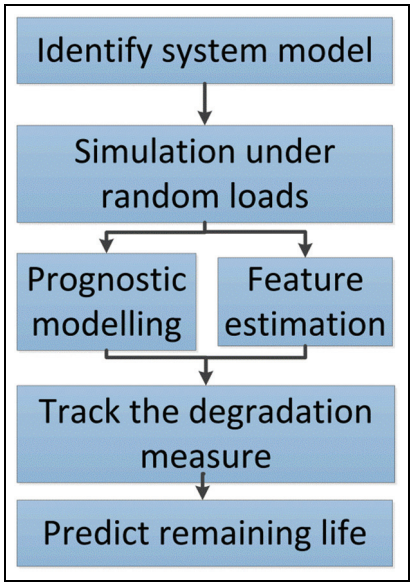


Figure 1. Physics-based approach.[25]

Downloaded from ade.sagepub.com at Cranfield University on September 22, 2016

degradation of the system, where random scenarios are simulated and compared to measurable data to identify the appropriate scenario (feature estimation) and estimate the RUL.

Normally, for diagnostics, a fault is detected by comparison between the outputs of the PbM and the measurements from the real system. An example of diagnostics using PbMs is the classification of bearing defects by measuring the natural frequencies of the components of the bearing, obtained from knowledge of the physics of the system, and deviations from normal values are used as health indicators as shown by Li et al.[26]

It should be noted that to develop prognostics capabilities, prior knowledge of the current health status of the system (diagnostics) is required. For prognostics based on PbMs, degradation models are used to represent the degradation mechanisms of the system and the RUL can be estimated as an output of these models. For instance, degradation models based on Paris law[27] to represent crack growth have been used by several authors to estimate the RUL of systems subject to fatigue.[14,28–33]

Health condition monitoring algorithms are normally classified into PbMs and DDMs, but the benefits of both approaches can be combined to obtain more robust algorithms called hybrid models. Orsagh et al.[34] proposed a generic framework (Figure 2) that used DDMs for diagnostics and a PbM for prognostics of bearings spalling by combining sensor data for diagnostics with model-based and historical data for prognostics. A similar approach is proposed by Zio and Di Maio,[14] who applied Paris law for crack growth estimation (prognostics) and a relevance vector machine method for fault detection (diagnostics), while Pantelelis et al.[15] were able to detect faults in a naval turbocharger combining finite element models of the system and an artificial neural network (ANN) for fault identification using vibration analysis.

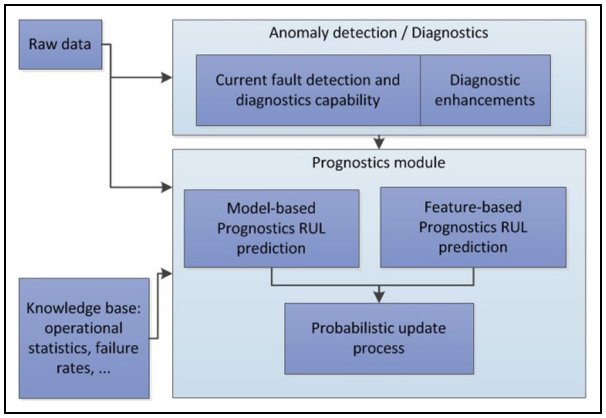


Figure 2. Hybrid model.[34]

For prognostics, regardless of the approach (PbM, DDM or hybrid), the health condition monitoring algorithm will provide an assessment of the current health of the system, normally by measuring a health indicator, and a prediction of the future health of the system. That prediction should be as accurate as possible, but there are always errors between the predicted value of a health indicator and the measured one. Thus, it is important to have the capability to adjust the model in order to minimize these differences based on the past errors between the predicted health indicator and the measured ones. PbMs can be combined with parameter estimators to minimize these errors in real time.[2] A unified formulation has been proposed by Jaw and Wang[35] to implement parameter estimators into PbMs given a generic set of system equations. The most common parameter estimators are shown in Table 1. Linear estimators are less computationally expensive, but if the system behaviour is clearly more sophisticated non-linear algorithms are needed.

Failure modes of rotating machinery

The development of PbMs requires an understanding of the system during normal operation and when a failure occurs. A failure is considered when a function of the system cannot be executed. It should be noted that 'failure mode' refers to the description of how a function of the system is no longer fulfilled, and a 'degradation mechanism' refers to the process that leads to a failure.[45]

The main contribution of this article is the review of potential degradation models that can be used for health condition monitoring. Those degradation mechanisms represent the phenomena behind a specific failure mode. This section describes relevant failure modes and their degradation mechanisms. A comprehensive review of those degradation mechanisms is given in the following section.

The most common failure modes of typical components of rotating machinery are analysed and current health condition monitoring algorithms are discussed; these algorithms are summarized in Table 2. Three typical components of rotating machinery are considered:

- Gears;
- Rolling bearings;
- Hydrodynamic bearings.

Table 1. Parameter estimators.

Linear estimators	Non-linear estimators
Least square[33,36,37]	Extended Kalman filter[19,29,38–40]
Linear Kalman filter[41,42]	Particle filter[28,31,43,44]

Downloaded from ade.sagepub.com at Cranfield University on September 22, 2016

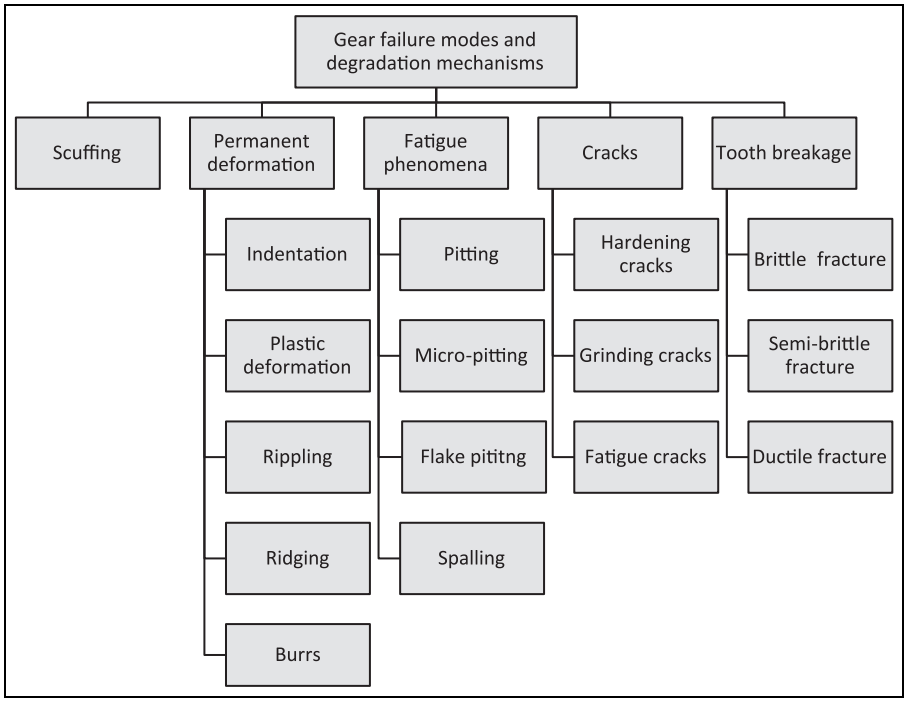


Figure 3. Gear damage terminology.

Table 2. Health condition monitoring algorithms classified by component and failure mode.

Gears	Bearings
Scuffing[46]	Fatigue: spalling/pitting[34,36,37,47–59]
Pitting[60–64]	Localized defects[65–69]
Crack detection[70,71]	Wear[72–74]
Crack length estimation[32,75–77]	Damage location[26,78–82]
Tooth breakage[11,62,83]	Geometrical imperfections[26,55]
	Contaminants[84]
	Metal–metal contact[85,86]

Gears

Gears are subjected to high cyclic loads and harsh environments, thus being able to monitor the health of the gears is of major importance. In this review, the failure modes of gears are classified following the guidelines of the ISO 10825:1995,[87] which classifies gear failures as shown in Figure 3. Each failure mode will be described and their corresponding PHM solutions will be briefly reviewed.

Scuffing (Figure 4(a)) consists in damage in the sliding direction due to metal–metal contact caused by insufficient lubrication, causing the subsequent transfer of material and increased vibrations and noise. Castro and Seabra[46] proposed a simplified model that does not consider surface parameters and a more sophisticated

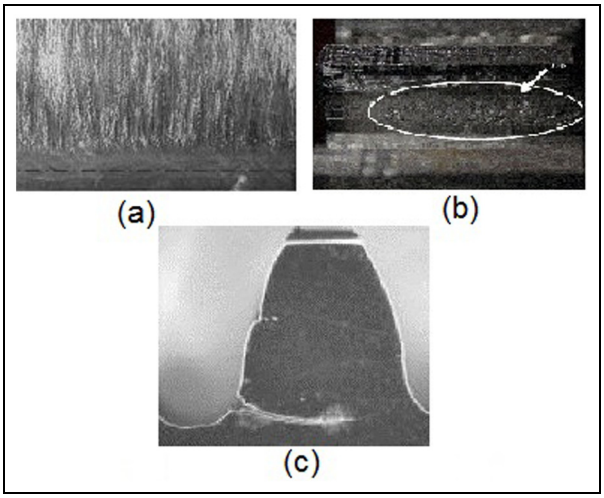


Figure 4. Gear defects: (a) scuffing,[46] (b) pitting[60] and (c) crack.[32]

mixed lubrication model that required roughness parameters to detect scuffing in gears under a variety of speeds, torques and oil bath temperatures. Therefore, scuffing can be modelled using wear models, in particular models that predict metal–metal contact between the teeth.

Permanent deformations include indentation and scratches that can be caused by foreign objects, or permanent deformation of the teeth. Permanent deformation consists of plastic deformation, which occurs

Downloaded from ade.sagepub.com at Cranfield University on September 22, 2016

under excessively high stresses; thus, excessive load can cause permanent deformations; the accumulated plastic deformation mechanism consists of low cycle fatigue (LCF).

The cyclic stresses produced in gears also cause high cycle fatigue (HCF), characterized by removal of material. This type of damage can be divided into pitting and spalling. Pitting consists of surface fatigue between rolling and sliding contacts, leading to small scattered holes as shown in Figure 4(b). If initial pitting is not detected, it can lead to spalling, which consists of macro-pitting caused by the association of small cracks into bigger ones.[87] The degradation mechanisms and the differences between pitting and spalling have been discussed in depth by Ding and Rieger.[88] Pitting and spalling are caused by stresses that do not lead to permanent plastic deformations; instead, the main degradation mechanism is driven by the high number of cycles for a relatively low load. This degradation mechanism is HCF.

Cracks (Figure 4(c)) are caused by defects in the gear due to deficient material properties, the manufacturing process or fatigue.[87] Crack detection has caught the attention of several authors and promising results have been obtained not only for diagnostics, but also for prognostics through the estimation of the crack length and its correlation with the RUL.

For diagnostics, simple DDMs as statistical parameters can be used as health status features. For instance, Zakrajsek and Lewicki[70] detected spur gear tooth cracks before complete fracture occurred using several statistical estimators. For prognostics of cracks, Feng et al.[75] used spectrum features to detect a crack and predict its evolution. However, the results were only based on simulations. A more common approach for prognostics consists of a PbM based on Paris law[27] to model the degradation mechanism and estimate the crack growth rate, which is an indicator of the RUL. Kacprzynski et al.[76] proposed the combination of Paris law along with a simplified two-dimensional (2D) finite element analysis (FEA) for RUL estimation. This approach was extended by Li and Lee,[32] who developed a dynamic model of a transmission to estimate the loads, a FEA to infer the stresses and an algorithm based on Paris law to obtain the RUL. The same approach was later used by Kacprzynski et al.[77] for prognostics of H-60 helicopter gear cracks using a more sophisticated three-dimensional (3D) FEA to estimate the loads, including crack initiation and crack propagation PbMs. Therefore, it is evident that the most suitable degradation models consist of representing crack growth.

Tooth breakage, total or partial, can have diverse causes and be produced by a single very high load or after a few cycles of high loads and the fracture can vary from ductile to brittle fracture.[87] Using vibration analysis, Wu et al.[83] differentiated between broken, worn or healthy teeth applying the support vector machine (SVM) technique. Partial breakage of the tooth, called chipping, can also be detected by looking at the differences in the mesh frequency side bands in the time–frequency domain.[11,62] This failure mode is caused by a single event; there is no continuous degradation from healthy to faulty conditions.

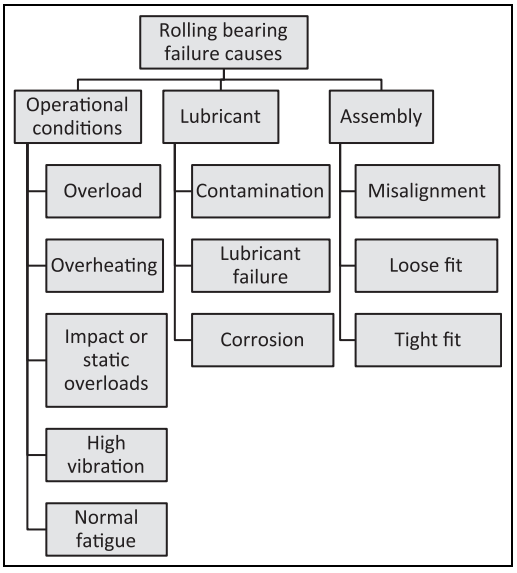


Figure 5. Damage causes in rolling bearings.

Bearings

Rolling bearings. Bearings are necessary to provide support for the rotating machinery, transmitting the axial and radial loads from the rotating component to the structure, and to minimize the friction losses in the sliding direction. This section will analyse rolling bearings, and hydrodynamic bearings will be covered in the next subsection. The failure modes are normally classified depending on the components that are damaged, differentiating between inner race, outer race, rolling elements and cage failures.[26,79,80]

The failure modes of rolling bearings can also be divided into failures caused by excessive operational conditions, by the lubricant and by assembly and disassembly errors[89] as shown in Figure 5.

Being able to detect lubrication anomalies, which are responsible of 50% of all the premature bearing failures in oil-lubricated bearings[90], would help to detect incipient failures by controlling the cause of the damage instead of the effect. Iyer et al.[91] reviewed the techniques available to detect lack of lubrication and contamination and stated that even if ferrous debris sensors and oil condition monitoring can provide very valuable information, they cannot be applied to oil bath lubricated bearings.

Downloaded from ade.sagepub.com at Cranfield University on September 22, 2016

Most of the research has been focused on detecting defects through vibration analysis and acoustic emission (AE). El-Thalji and Jantunen[92] stated that bearing faults are assumed to produce impulses that affect the vibration spectrum and conducted an extensive review of the state of the art of PHM of rolling bearings covering bearing faults, monitoring techniques and signal processing methods. Previous reviews of health monitoring of rolling bearings can also be found.[93–96]

Sunnersjö[55] studied the changes in the vibration response of rolling bearings subjected to geometrical imperfections, spalling and abrasive wear using time-history diagrams, spectrograms and time–frequency analysis. Spalling also was studied by Sawalhi and Randall[56] using vibration analysis and time–frequency analysis to take into account the low-frequency spectrum of the incipient spalling and the high-frequency impulsive response of severe spalling. The effect of contaminants in the vibration response of rolling bearings is analysed by Maru et al.,[84] who found significant differences in root mean square (RMS) values for frequencies between 600 and 10,000 Hz and compare the effect of contaminants using different particle sizes.

AE techniques have also proven to be effective in detecting defects in lubricated sliding contacts, including rolling and hydrodynamic bearings. Boness and McBride[74] found an empirical relationship between AE, RMS and wear volume removed. An effect caused by adhesive and abrasive degradation mechanisms in lubricated point contacts. Price et al.[58] used AE and vibration analysis in the time and frequency domain showing the potential of AE to detect incipient pitting with a high signal-to-noise (S-N) ratio. Guo and Schwach[59] studied the effectiveness of AE parameters to detect rolling contact fatigue in point contacts, finding that RMS and amplitude were the better indicators of surface defects. Rahman et al.[50] were able to detect and localize incipient fatigue damage in rolling contacts using the AE hit count rate. Choudhury and Tandon[66] detected incipient inner race and roller bearing faults by measuring AE counts. He et al.[67] applied a more sophisticated technique, the wavelet scalogram in the time–frequency domain, to detect defects in rolling element bearings using AE under different operational conditions.

AE has also proven effective in detecting microcracks in the surfaces of axial bearings earlier than with vibration analysis by looking at the hit count rate and the amplitude of the signal.[51,52] Elforjani and Mba[53] also detected and located fatigue damage in axial bearings using AE. Jamaludin and Mba[68,69] proved that AE is a powerful technique to detect damage of rolling bearings at extremely low speeds.

Less common techniques have also been used and compared to vibration and AE analysis. For instance, Kim et al.[65] compared vibration analysis with ultrasounds using statistical parameters in the time domain and spectral analysis to detect damage in rolling bearings and obtained better results using ultrasounds for low bearing speeds. Sun et al.[72] compared AE and an electrostatic wear monitoring method that measures the electrical charge in the bearing and correlated it with the wear degradation finding that both techniques are able to detect wear caused by metal–metal contact. Harvey et al.[73] also validated an electrostatic wear detection method for rolling contacts able to detect seeded faults prior the total failure occurred.

Regarding the health condition monitoring algorithms, machine learning also proved to be a useful approach commonly used for fault classification. Paya et al.[78] obtained features from the wavelet transform, later used for training and testing an ANN capable of differentiating between bearing faults in the inner race of the bearing and faults in the adjacent gears; while Jack and Nandi[80] compared bearing features from time and frequency domains by combining an ANN and a SVM algorithm to detect inner race, outer race, ball and cage faults. Li et al.[26] used the frequency domain of the vibration signal from rolling bearings to detect ball and inner race damage along with looseness using the fundamental bearing frequencies as features to train an ANN. Tang et al.[79] also detected cracks in bearings and classified them as ball, inner race or outer race crack with 92% accuracy in a wind turbine transmission using a SVM algorithm. Du et al.[81] also differentiated between ball, inner and outer race failures using a modified SVM algorithm with 94% accuracy.

Health condition monitoring algorithms based on PbMs are not too many when compared to DDMs. However, there are important examples of PbMs for rolling bearings. McFadden and Toozhy[47] detected spalling using a PbM that calculates the characteristic frequency of damage caused by spalling and synchronously averaged the frequency response with the rotating speed of the shaft and was able to detect spalling and estimate the distribution of the damage in the inner race. Zong et al.[97] developed a PbM to identify spalling in the inner rig using a FEA model of the defect and its vibration response. Another important PbM for prognostics of rolling bearings was introduced by Li et al.,[37] who were able to estimate the RUL as a function of the size of the spalls using a deterministic degradation model similar to Paris law, further improved to include the stochastic of the failure.[36] Orsagh et al.[34] later applied a similar approach to detect spalling and estimate the RUL in rolling bearing. Qiu et al.[48] proposed a different PbM approach to detect damage in bearings, consisting in a dynamic model of the bearing that correlates the natural frequencies and their amplitude, obtained from the vibration response, with the stiffness of the system. This approach is later integrated with a degradation model that defines the damage as a

Downloaded from ade.sagepub.com at Cranfield University on September 22, 2016

Table 3. Major causes of premature hydrodynamic bearing failure.

Major causes of premature bearing failure	
Dirt	45.4%
Incorrect assembly	12.8%
Misalignment	12.6%
Insufficient lubrication	11.4%
Overloading	8.1%
Corrosion	3.7%
Improper journal finish	3.2%
Other	2.8%

function of the stiffness and can be used to estimate the RUL of the bearing. However, Sun et al.[82] argue that methods based on characteristic frequencies are not accurate enough and proposes a DDM based on fuzzy logic to classify outer race, inner race and ball bearing faults with 94.7% accuracy.

Different rolling failure modes have been analysed. Some failure modes, such as contaminants and geometrical imperfections, are caused by external factors and degradation mechanisms cannot be modelled, because the particle size or composition of contaminants and the dimensions of the geometrical imperfections are unknown. Fault isolation techniques to differentiate between inner/outer or ball failures lead to wear of the faulty sub-component; the fundamental frequencies of the components can be modelled and monitored to localize the failure. In order to track spalling and pitting in rolling bearings, as it occurs with gears, the degradation mechanism consist of fatigue due to excessive cycles and loading. HCF models and spalling growth models, similar to Paris law can be used.

Hydrodynamic bearings. The function of hydrodynamic bearings and rolling bearings is identical: to provide low friction in the sliding direction and to transmit the radial and axial loads. The main difference is the type of contact, in which both surfaces slide without any intermediate component.

The most typical failure modes of hydrodynamic bearings[98] are shown in Table 3. Zeidan and Herbage[99] also reached the same conclusions after analysing the most common failures of hydrodynamic bearings.

Dirt, incorrect assembly and defects in the manufacturing process are particularly difficult to monitor. Thus, most of the research has been focused on detecting insufficient lubrication, which is directly related to metal–metal contact and leads to rapid degradation. The main failure mechanism related to insufficient lubrication is scuffing, already discussed for gears, which eventually develops into seizure.[100] Tanaka[101] demonstrates experimentally the effect of flow rate and speed in the lubrication phenomena by measuring eccentricity and cavitation under insufficient

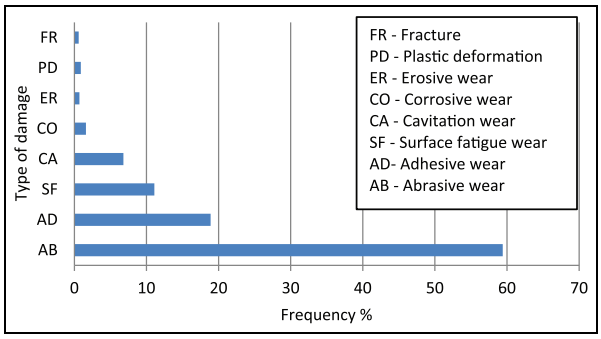


Figure 6. Percentage occurrence of types of hydrodynamic bearing damage.[103]

lubrication compared to fully flooded lubrication. Even if a film of lubricant remains and there is not metal–metal contact, fatigue damage can occur due to the cyclic stresses on the surface of the bearing as shown by Huang et al.,[102] who studied fatigue wear in hydrodynamic bearings.

A variety of failure analysis of hydrodynamic bearings can be found in the literature. Vencl and Rac[103] studied the failures of over 180 engine bearings, finding that abrasive wear is the predominant degradation mechanism, followed by adhesive and fatigue wear, as shown in Figure 6. They also identified the causes corresponding to each degradation mechanism:

- Contaminants in the lubricant: provoke abrasive wear;
- Overload: provokes fatigue wear caused by excessive stresses on the surfaces of the bearing;
- Insufficient clearance: provokes adhesive wear;
- Insufficient lubrication: provokes adhesive wear;
- Metal–metal contact: provokes adhesive wear.

A comparison between temperature measurements, electric resistance, vibration analysis and metallic particle measurements for detecting metal–metal contact has been conducted by Okamoto et al.,[85] proving the following:

- Vibration analysis at high frequencies can detect metal–metal contact.
- Temperature analysis yields good results, but its sensitivity depends on the location of the sensor.
- Electrical resistance and debris analysis are effective in detecting metal–metal contact.

Moosavian et al.[86] used vibration analysis to detect oil starvation using ANNs while a less common technique, AE, has also proven successful for detecting metal–metal contact.[104] It should be noted that research on wear and fatigue detection of sliding contacts can also be applied to hydrodynamic bearings taking into consideration line contact instead of point contact.

Downloaded from ade.sagepub.com at Cranfield University on September 22, 2016

Table 4. Gears failure modes, degradation mechanisms and potential PbMs.

Failure mode	Degradation mechanism	PbM
Scuffing	Wear, metal–metal contact	Stribeck curve, mixed lubrication model
Permanent deformation	Excessive loading leading to plastic deformation	Low cycle fatigue, structural analysis
Pitting and spalling	Excessive cycles/load	High cycle fatigue
Cracks	Excessive cycles/load	Crack growth model (Paris law)
Tooth breakage	Single event (excessive load)	Structural analysis

PbMs: physics-based models.

Table 5. Bearings failure modes, degradation mechanisms and potential PbMs.

Failure mode	Degradation mechanism	PbM
Inner/outer/ball failure (rolling bearing only)	Wear	Fundamental frequencies model to identify faulty sub-component
Spalling/pitting/cracks	Excessive cycles/load	Spalling growth estimation model/stiffness model changes in frequency spectrum
Insufficient lubrication	Wear, metal–metal contact	Stribeck curve, mixed lubrication model

PbMs: physics-based models.

As it occurs with rolling bearings, many failure modes cannot be modelled based on their degradation mechanism because the parameters of the degradation mechanism are unknown, for example, dirt, incorrect assembly, misalignment, geometrical imperfections. However, the underlying degradation mechanisms of some important failure modes can be modelled and used for PHM. Insufficient lubrication, which leads to scuffing, is caused due to wear in the contact between the journal and the support. This failure mode can be monitored with a degradation model capable of modelling the wear and friction in the contact.

Failure modes and their degradation mechanisms

PbMs describe the phenomena of a system under healthy and faulty conditions. They have the potential to assess the health of the system (diagnosis) and predict the RUL by tracking the degradation of the system. Therefore, the degradation mechanisms and their correspondent models of a failure mode should be identified in order to develop prognostics capabilities based on PbMs.

However, degradation models require inputs to estimate the severity of the deterioration of the system and feedback about the current degradation particularly for prognostics. This information is obtained through sensors, known operational conditions and measured or known environmental conditions.

A common challenge when PbMs are developed is that the inputs of the degradation model are 'internal loads' that are not always measured directly. Instead, there is information about 'external loads'.[45] A PbM is required to relate the external and internal loads, plus the degradation model that assesses the health of the system. Therefore, not only a degradation model is needed, but also a PbM relates the measured variables with the inputs of the degradation model.

Some of the failure modes described in the previous section can potentially be modelled using PbMs. Tables 4 and 5 summarize the type of degradation models that can be applied to each failure mode. Additional models to relate external and internal loads are also included.

Relevant degradation models

The importance of representing accurately the physics of the system has already been mentioned in previous sections. This section reviews the models of the most relevant degradation mechanisms of rotating machinery. Common failure modes of rotating machinery and their corresponding degradation mechanisms were identified. The aim of this section is to serve as a tool to select the most appropriate models to represent these mechanisms. Additionally, the understanding of the most critical variables and parameters of each degradation mechanism will help to identify what phenomena should be monitored. The following degradation mechanisms are covered:

- Creep;
- Fatigue;
- Fatigue and creep;
- Wear.

Downloaded from ade.sagepub.com at Cranfield University on September 22, 2016

Table 6. Health condition algorithms based on PbMs.

Creep	Fatigue	Creep and fatigue	Wear
Baraldi et al.,[19,44] Chin[105] and Yu and Zhou[106]	Fatigue[48,77] Cracks[14,28–32,113,114] Spalling[35,37,119–123]	Vogel et al.,[107] Daroogheh et al.,[108] Bray et al.,[109] Wu et al.[110] and Tinga et al.[111]	General wear[112] Fretting[115–118] Metal–metal contact[46,124,125]

PbMs: physics-based models.

The amount of health condition monitoring algorithms based on PbMs is limited, as opposed to DDMs. PbMs are not scalable between different systems; additionally, they require a good understanding of the phenomena behind a failure mode. However, health monitoring using PbM is particularly useful in prognostic algorithms due to their potential to estimate the current and future health of the system based on degradation models. The models described in this section are summarized in Table 6.

Creep

Creep consists of a permanent deformation that can be caused by low loads under high temperature due to the formation of voids in the grain boundaries (GBs) of the material that extends until it becomes inter-granular and fracture occurs. The creep phenomenon is time and temperature dependent. Creep is divided into three stages depending on the creep rate, defined in equation (1), where ε is the deformation and t is the time:[126]

- First stage: initially, there is primary creep, with a decelerating creep rate.
- Second stage: stable minimum creep rate, called secondary creep, which covers most of the time.
- Third stage: creep rate, called tertiary creep, accelerates until fracture occurs.

$$\text{Creep rate} = \frac{\Delta\varepsilon}{\Delta t} \tag{1}$$

The Larson Miller parameter (LMP), shown in equation (2), is commonly used to characterize creep behaviour, reducing the problem from two variables, time and temperature, to only one: the LMP. The correlation between maximum stress and LMP depending on the material can be obtained experimentally. However, this equation is purely experimental and does not rely on the physics of the degradation mechanism. It also implies constant temperature along time. Thus, for variable conditions, a cumulative damage rule is required. For instance, a parameter D can be used if stress and temperature levels vary over time to take into account the damage on each instant as shown in equation (3), where Δt_i is the duration of a constant loading period and $\Delta t_{r,i}$ is the rupture time for the given loading condition, obtained from equation (2). The failure is estimated when D is above 1[60]

$$\text{LMP} = (T(^\circ F) + 460) \times (20 + \log_{10}(t)) \times 10^{-3} \tag{2}$$

$$D = \sum_{i=1}^{n\,periods} D_i = \sum_{i=1}^{n\,periods} \frac{\Delta t_i}{\Delta t_{r,i}} \tag{3}$$

Instead of using the LMP, a physics-related model that is commonly used to represent creep behaviour is Norton creep law, as shown in equation (4), where σ is the stress level; T is the temperature; and A, n and p are material constants. It should be noted that Norton creep law is only able to represent the second stage of creep behaviour and does not consider material behaviour at a microscopic level.[45] More complex models that take into account these effects are able to estimate the first and third stages as well[127,128]

$$\text{Creep rate} = AT^n\sigma^m \tag{4}$$

The application of creep models for health condition monitoring has been focused on hot sections of turbine blades. Chin[105] proposed a prognostic approach that estimates the RUL of turbine blades based on a creep model that estimates the stresses based on temperature and time. A similar approach was applied by Baraldi et al.[19,44] to predict creep degradation of turbine blades based on Norton law and Particle Filter (PF) or a Kalman filter for parameter estimation; however, only simulated data were used. Yu and Zhou[106] proposed a creep model based on FEA and the Kachanov–Rabotnov (K-R) model[129,130] to assess damage of high temperature threaded joins by taking into account the damage due to stress relaxation and reduced preload instead of using permanent deformation as the health indicator.

Fatigue

Fatigue occurs in systems subject to cyclic loading, due to thermal and mechanical stresses. The degradation mechanism differs between HCF and LCF. HCF stresses are below the yield stresses and $\Delta\sigma$ (stress range) is the factor that controls the degradation mechanism. However, for LCF, the stress level is above the yield

Downloaded from ade.sagepub.com at Cranfield University on September 22, 2016

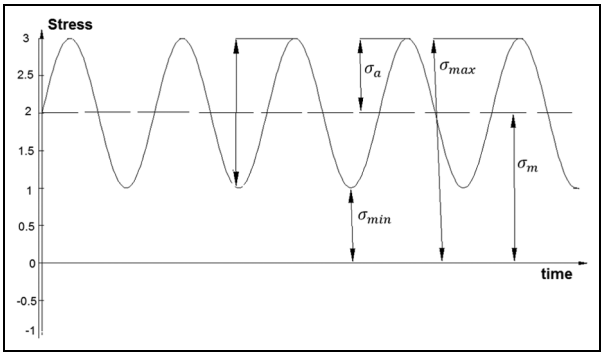


Figure 7. Fatigue parameters.

stress limit and there is plastic deformation. Thus, $\Delta\varepsilon$ (strain range) is the magnitude that controls the degradation.[45]

For HCF, Wöhler[131] demonstrated that the cyclic stress range is the driven factor of fatigue degradation based on experimental fatigue data of railroad axles; thus, it should be represented using S-N curves that correlate the number of cycles and a characteristic stress level. The use of experimental S-N curves can be used for life prediction of metallic structures subject to fatigue. Analytical equations for the appropriate metallic structure can be found in well-accepted standards such as the British Standard 7608:2014,[132] which also provides the standard deviation as shown in equation (5), where N_f is the number of cycles; σ_a is the stress amplitude; SD is the allowed standard deviation; and C_o, d and m are parameters dependent on the geometry.

Apart from the stress range, the mean stress σ_m is also an important factor that has to be taken into account, which is normally described as a stress ratio $R = \sigma_{max}/\sigma_{min}$. The relation between all these variables is shown in Figure 7.

Basquin law[133] proposed a stress-based analytical equation based on the experimental work of Wöhler,[131] as shown in equation (6), where N_f also refers to the number of cycles, σ_a is the stress amplitude, σ'_f is the fatigue strength coefficient and b is the fatigue strength exponent. It should be noted that any discontinuity in the material, bad surface quality or internal stresses negatively affect the life of the component.[45] These detrimental factors are particularly critical under high temperatures as shown by Boardman,[134] who studied the detrimental effect of higher temperature and notches in the fatigue life of a variety of alloys.

$$\log(N_f) = \log(C_0) - d \times SD - m \times \log(\sigma_a) \quad (5)$$

$$\sigma_a = \frac{\Delta\sigma}{2} = \sigma'_f(2N_f)^b \quad (6)$$

For LCF, plastic deformation is the main factor that controls the failure mechanism; Manson–Coffin law is commonly used to represent this degradation mechanism.[135,136] This method considers that cyclic life depends on the deformation using a power law as shown in equation (7), where $\Delta\varepsilon_p$ is the plastic strain range and c and ε_f are experimental constants. A more accurate model, the Manson and Halford model, considers the elastic and plastic component of the strain, thus being able to represent LCF and HCF degradation mechanisms, as shown in equation (8), where D represents the ductility, σ_u is the ultimate tensile strength and E is the Young's modulus.[126] Kacprzynski et al.[76] evaluated the plastic strain of a helicopter gear tooth using an FEA model and later applies Manson–Coffin law to evaluate the number of cycles until crack initiation occurs.

$$\Delta\varepsilon_a = \frac{\Delta\varepsilon_p}{2} = \varepsilon_f(2N_f)^c \quad (7)$$

$$\Delta\varepsilon = D^{0.6} \times N_f^{-0.6} + \left(\frac{3.5 \times \sigma_u}{E}\right) \times N_f^{-0.12} \quad (8)$$

A cumulative damage rule is required to take into account variable loading conditions. The simplest and a well-accepted approach were proposed by Miner,[137] as shown in equation (9), where D is the cumulative damage, n_i are the current number of cycles under the actual loading condition and N_i are the number of cycles until failure, which is estimated if D is above 1. It should be noted that this approach considers the RUL independent of the order of the loads. Similar equations can be used to represent different types of cumulative damage. For instance, Qiu et al.[48] proposed a similar cumulative rule that is a function of the stiffness of the system instead of the number of cycles

$$D = \sum_{i=1}^{load\ p} \frac{n_i}{N_i} \quad (9)$$

Cracks are a common consequence of fatigue damage, and the degradation mechanism that ultimately leads to failure due to fracture of the component. The previous models do not consider the physics that lead to the fracture and only rely on empirical results. An alternative approach is to predict the failure based on fracture mechanics. Crack growth is divided into three regions:[45]

- First region: slow crack growth and the crack length is not considered significant;
- Second region: the crack growth rate becomes significant and constant;
- Third region: the crack becomes unstable and the propagation rate increases until fracture occurs.

The initial length and the propagation rate of the crack can be estimated and used as an indicator of the

Downloaded from ade.sagepub.com at Cranfield University on September 22, 2016

RUL of a system subject to fatigue. The most widely accepted model for crack growth, the Paris law, was proposed based on experiments that proved the correlation between crack length and number of cycles by Paris et al.,[27] as shown in equation (10), where a is the crack length; N is the number of cycles; m and b are parameters of the material; and K is an intensity coefficient that depends on the geometry and type of crack. A similar equation introduced by Hoeprich[121] can be used to represent spall area growth in bearings, as shown in equation (11), where D is the defect area, C_0 and n material parameters, validated with experimental results by Li et al.[122] and further improved to consider thermal effects by Kotzalas and Harris.[123] It should be noted that specific degradation models can also be used for prognostics. For instance, the rolling contact fatigue model proposed by Sadeghi et al.[138] based on the crack propagation and crack initiation has the potential to be used for PHM

$$\frac{da}{dN} = m\Delta K^b \tag{10}$$

$$\frac{dD}{dN} = C_0 D^n \tag{11}$$

Paris law represents the second region of crack growth but does not take into account the initial crack length and the instability of the crack. However, for PHM, being able to represent only the second region of the crack growth using Paris law has proven sufficient to model the degradation of the system. This is shown by Corbetta et al.,[28] who estimated the crack growth on structures and the uncertainty of the prediction combining the PbM with PF for parameter estimation. Ray and Tangirala[29] also estimated the RUL based on Paris law but using a Kalman filter for parameter estimation. Orchard et al.[30] applied both PF and an extended Kalman filter (EKF) on a crack growth model based on Paris law to estimate crack length in the plate of the gearbox of a helicopter. Pais and Kim[114] developed a fatigue crack growth PbM for prognostics of aerospace panels by computing a FEA model and a fatigue crack growth model as a function of the usage history, a modified Paris law to consider variable amplitude loads was used.

Zio and Di Maio[14] combined Paris law with a SVM algorithm to select the appropriate degradation model to estimate crack length. Oppenheimer and Loparo[31] also calculated the RUL of rotor shafts due to cracks using Paris law, while Li and Lee[32] combined a dynamic model that estimates the stresses on a gear with Paris law to represent the degradation to estimate the RUL of the gear. A more sophisticated algorithm is proposed by Kacprzynski et al.,[76] who estimated the RUL of helicopter gears by modelling the first region (crack initiation) using Manson–Coffin law presented above to estimate the number of cycles until a crack initiates and using Paris law to estimate the crack growth afterwards. The spall degradation formula presented in equation (11) has been applied for RUL estimation of rolling bearings by Orsagh et al.[34] and Li et al.,[36,37] while Slack and Sadeghi[120] developed a more sophisticated explicit finite element (FE) spalling model that predicts the number of cycles until failure by modelling the crack initiation in the sub-surface and its propagation. For diagnostics, Fu and Gao[113] developed a PbM capable of estimating the natural frequency response of a crack in a fan blade assessing its size and location.

Creep and fatigue

When alternative loads are coupled with creep deformation, both degradation mechanisms, creep and fatigue, interact with each other and cannot be treated independently.[45] The most relevant method to represent this behaviour is strain range partitioning (SRP).[139] The SRP method assumes that different strain ranges produce different hysteresis loops and differentiates between two types of deformation: GB sliding and attendant slip plane (SP) sliding; the former is considered when creep is the main failure mechanism and applies to slow cycles, and the latter applies to degradation caused mainly by fatigue, consisting of deformation due to cyclic loading.[126] Depending on the type of the strain during the tension and compression phase of the hysteresis loop, four possible scenarios can occur as shown in Figure 8. Once the scenario is identified, the number of cycles to failure can be obtained as a

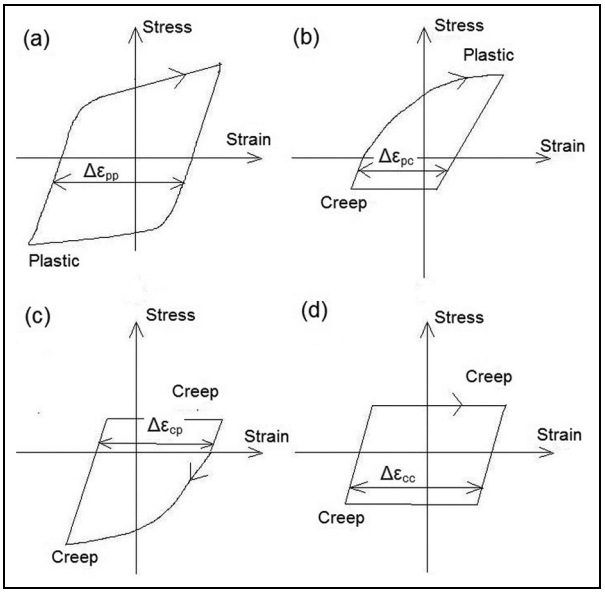


Figure 8. Four SRP hysteresis scenarios: (a) PP, (b) PC, (c) CP, (d) CC, where P refers to plastic strain and C refers to creep strain during tension and compression phases.

Downloaded from ade.sagepub.com at Cranfield University on September 22, 2016

function of the strain range. Vogel et al.[107] used the SRP method to predict crack initiation in a jet engine's combustor liner and correlate them with experimental results.

However, the SRP method is not the only valid approach. Daroogheh et al.[108] modelled the creep–fatigue behaviour of turbine blades considering both mechanisms independent of each other and calculated the cumulative damage using the rain flow method. Bray et al.[109] used a FEA approach that incorporates creep and fatigue routines to calculate damage in pipe joints. Complex models that take into account the microstructure of the material can also be used to obtain more accurate results as the framework proposed by Wu et al.[110] Tinga et al.[111] developed a degradation model of creep–fatigue that estimated the number of cycles until failure for single crystal Ni-based alloys, obtaining adequate agreement with experimental results.

Wear

Wear, also referred to as abrasion and scuffing, is a degradation mechanism caused by friction between two sliding surfaces associated with loss of material, including damage due to direct contact between the surfaces and damage caused by the fluid between the surfaces.[45] However, the modelling of wear is particularly challenging due to the high influence of external factors that affect the contact such as the environment.[118] Wear can also be considered as a dissipation of energy mainly controlled by friction,[140] and it is classified as follows: adhesive and abrasive (depending on the hardness of the materials in contact[141]), corrosive, thermal and fatigue wear.[112]

Adhesive wear can be modelled using Archard's law, as shown in equation (12), where V_{wear} is the wear volume, H is the material hardness, W is the load, L is the sliding distance and K is the wear coefficient. Using this law, more complex wear models can be obtained by modifying the value of the constant K, as shown by Watson et al.,[112] who applied variants of Archard's law to represent adhesive, abrasive and corrosive wear

$$V_{wear} = K\left(\frac{WL}{3H}\right) \tag{12}$$

Fatigue wear leads to cracks initiated below the surface. After a number of cycles these cracks develop into pitting or spalling with the subsequent removal of material. A degradation model for wear caused by subsurface fatigue has been proposed by Ghosh et al.,[142] who provided an experimental correlation between wear and crack propagation, which is a function of the shear stress on the surface as shown in equation (13), where N is the number of cycles to failure; a and b are empirical constants; and Q is the contact shear stress that depends on the friction coefficient and load applied

$$\log(N) = a \cdot \log(Q) + b \tag{13}$$

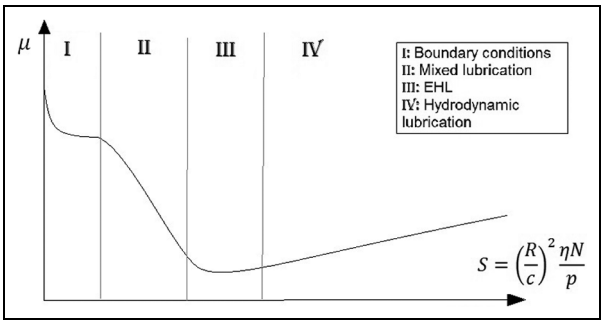


Figure 9. Qualitative Stribeck curve: friction (μ), Sommerfeld number (N: speed, p: load, η: dynamic viscosity of the lubricant, R: radius of the bearing, c: clearance of the bearing).

However, wear is controlled by Friction. Therefore, more accurate models should predict the friction between the sliding surfaces as well. The friction force is defined as the opposing force to the motion of a body to another and depends on the normal force and the friction coefficient. For non-lubricated contacts, Coulomb law[143] can be applied, considering the friction coefficient constant and independent of the speed and load, as shown in equation (14). Where F_T is the friction force, μ is the friction coefficient and F_N is the normal force, but for lubricated contact in motion hydrodynamic theory must be applied

$$F_T = \mu F_N \tag{14}$$

For lubricated sliding contacts, the friction is divided into four regions depending on the type of contact as shown in Figure 9: hydrodynamic lubrication, elasto-hydrodynamic lubrication (EHL), mixed lubrication and boundary lubrication, where the friction coefficient is represented as a function of a lubrication parameter, the Sommerfeld number S, which includes the effect of speed, load and viscosity.

Hydrodynamic contacts in rotating machinery, typically rolling and hydrodynamic bearings, are designed to operate on the hydrodynamic region, where the contact is fully lubricated and the friction forces are exclusively caused by the shear stresses of the lubricant. The fluid can be considered laminar and a simplified version of the Reynolds equation[144] using dimensionless parameters can be integrated along the bearing to calculate the film thickness and pressure distribution as shown in equation (15), where h^* is the dimensionless film thickness, p^* is the dimensionless pressure, x^* is the radial coordinate, y^* is the axial coordinate; and R and L are

Downloaded from ade.sagepub.com at Cranfield University on September 22, 2016

the dimensionless radius and length, respectively.[145] The friction force is calculated by integrating the shear stress τ along the bearing area as shown in equation (16), which requires the lubricant speed gradient on the surface, as shown in equation (17), thus obtaining the friction force as a function of the film thickness (18), where U is the relative speed and η is the dynamic viscosity

$$\frac{\partial}{\partial x^*}\left(h^{*3}\frac{\partial p^*}{\partial x^*}\right)+\left(\frac{R}{L}\right)^2\frac{\partial}{\partial y^*}\left(h^*\frac{\partial p^*}{\partial y^*}\right)=\frac{\partial h^*}{\partial x^*} \tag{15}$$

$$F=\int_0^{L}\int_0^{totalarc}\tau dxdy=\int_0^{L}\int_0^{totalarc}\eta\frac{\partial u}{\partial z}dxdy \tag{16}$$

$$\frac{\partial u}{\partial z}=\frac{U}{h} \tag{17}$$

$$F=\int_0^{L}\int_0^{totalarc}\frac{U\eta}{h}dxdy \tag{18}$$

For plain journal bearings, the film thickness h can be obtained as a function of the geometry and the eccentricity ratio ε, as shown in equation (19), where c is the clearance and θ is the radial angle. Thus, an analytical solution of the Reynolds equation (15) is obtained (equation (20)), where p is the pressure distribution as a function of the radial angle θ, the relative speed between the sliding surfaces U, the eccentricity ratio ε, the axial position y, the dynamic viscosity η and geometrical parameters: radius R, clearance c and bearing length L. The friction force can be obtained analytically as shown in equation (21).[145] Alternatively, Sinanoglu et al.[146] successfully estimated the pressure variations of a journal bearing using an ANN, but several pressure sensors along the bearing were required to train the network

$$h(\theta)=c(1+\varepsilon\cdot\cos(\theta)) \tag{19}$$

$$p=\frac{3\cdot U\cdot\eta\cdot\sin(\theta)}{R\cdot c^2(1+\varepsilon\cdot\cos(\theta))^3}\left(\frac{L^2}{4}+y^2\right) \tag{20}$$

$$F=\frac{2\pi\eta ULR}{c\sqrt{(1-\varepsilon^2)}} \tag{21}$$

The EHL regime applies under heavily loaded conditions. The deformation of the bearings caused by the load significantly affects the film thickness and should be considered by the model. Thus, a structural analysis is required to calculate the radial deformation along the bearing $d(\theta,y)$ caused by the pressure filed and should be included in the calculation of the film thickness as shown in equation (22). EHL models have been used for estimating the minimum film thickness based on operational conditions, as shown by Choi et al.,[147] who combined a multi-flexible dynamic model of the bearing with an EHL model that calculates the pressure distribution and film thickness

$$h(\theta,y)=c(1+\varepsilon\cdot\cos(\theta))+d(\theta,y) \tag{22}$$

An alternative approach is to use computational fluid dynamics (CFD) for hydrodynamic lubrication and to combine it with computational structural analysis for EHL. Stefani and Rebora[148] developed a CFD model that takes into account the wall convection, the thermo-mechanical deformations and the mixing phenomena in the groove, while Jin and Zuo[149] also used a CFD model to study the effect of different groove depths in journal bearings.

Mixed lubrication refers to the region in which partial metal–metal contact occurs and part of the load is transmitted by asperities. In this situation, surface parameters must be taken into account and the complexity and quantity of unknown parameters increase. Gelinck and Schipper[150] have developed a mixed lubrication model for line contacts which was later improved and validated for point contacts by Liu,[151] and which agreed with experimental results as shown by Lu et al.[152] The mixed lubrication model first calculates the film thickness and applies the mixed lubrication model if $h<h_{lim}$ is true; otherwise, the contact is considered hydrodynamic, h being the minimum film thickness and h_{lim} the limit at which mixed lubrication occurs. The mixed lubrication model assumes a percentage of the load transmitted through asperities, δ_2, and compares the pressure distribution transmitted through the asperities with the pressure distribution considering a Hertzian contact; δ_2 is updated until equation (23) converges, where $F_{3/2}$ is illustrated in equation (24), $\bar{n}$ is the dimensionless density of asperity summits, $\bar{\sigma}_s$ is the dimensionless standard deviation of the asperity height distribution, W is the load, A is the apparent contact area, p_{max} is the maximum Hertzian pressure and Φ_s^* is the standardized Gaussian distribution

$$\frac{2}{3}\bar{n}\bar{\sigma}_s^{3/2}F_{3/2}\left(\frac{h}{\bar{\sigma}_s}\right)=\frac{W}{A\delta_2 p_{max}} \tag{23}$$

$$F_{\frac{3}{2}}(\varphi)=\int_{\varphi}^{\infty}(s-\varphi)^{\frac{3}{2}}\Phi_s^*(s)ds \tag{24}$$

The Greenwood and Williamson[153] asperity contact model was used to calculate the load transmitted through the asperities, by considering spherical summits with a height that follows a Gaussian distribution subject to elastic deformation.

Under mixed lubrication, the friction coefficient is calculated as a function of the shear stress of the lubricant for the load transmitted through the lubricant (equation (16)) and using Coulomb law (equation (14))

Downloaded from ade.sagepub.com at Cranfield University on September 22, 2016

for the load transmitted through the asperities as shown in equation (25), where μ is the friction coefficient, μ_c is the friction coefficient for a dry contact, F is the friction force, W is the load and τ is the shear stress of the lubricant

$$\mu = \frac{F}{W} = \frac{\mu_c W \delta_2 + \int_0^{L\ total\ arc} \int_0^{} \tau dx dy}{W} \quad (25)$$

Faraon[154] presented a similar approach for line contacts further improved for starved contacts by Faraon and Schipper.[155] For point contact, Hua et al.[156] developed a mixed lubrication model that calculates the film thickness, pressure and temperature along the contact considering conductive thermal effects and stated the potential of the mixed lubrication model for scuffing prediction. Hu and Zhu[157] did not take into account the thermal effects but included the surface deformation in the calculation of the film thickness for EHL and mixed lubrication. A similar approach was used to detect scuffing in gears using a mixed lubrication model by Castro and Seabra.[46] Wang et al.[158] developed a mixed lubrication model that evaluates the influence of misalignment in hydrodynamic bearings under severe conditions that was validated using temperature data and stresses the influence of surface parameters when the film thickness is of the same order of magnitude as the roughness of the surface. Under boundary conditions, the lubricant does not transmit any of the load, and Coulomb and dry contact models are more suitable.

Stribeck curve modes can be applied to any lubricated contact, point contact models are normally used for ball rolling bearings, whereas line contact models are used for hydrodynamic and roller bearings. However, Wang et al.[159] developed a Stribeck curve model validated with experimental results for deep-groove ball bearings by calculating the torque produced by elastic hysteresis, hydrodynamic lubrication, slip, and friction between balls, cage and guiding lands using a complete different approach based on the energy lost.

PbMs for PHM based on degradation caused by wear are limited. However, the techniques to model wear presented above have the potential to be applied to PHM. Wear models have been used by Zhang et al.[160] to detect failures in piston bearings as a function of temperature, friction and roughness.

A variant of wear fatigue, called fretting, is associated with the small amplitude oscillatory motion between two solid surfaces in contact.[115] Leonard et al.[116] modelled a fretting in a line contact and calculate the severity of wear as a function of the number of cycles using Coulomb law (equation (14)) to represent the friction, a FE to represent the stresses and Archard's law to take into account the cumulative damage. Kasarekar et al.[117] evaluated the fretting fatigue life depending on the roughness of the surfaces in contact estimating the crack initiation using the Smith Watson Topper fatigue theory and Archard's law to model the wear. Quraishi et al.[118] also calculated the fretting fatigue life as a function of friction and loading using the Ramberg–Osgood equation and validated it with experimental results, while Walvekar et al.[115] also validated a fretting model that consists of a FEA model that computes the stresses and strains during each cycle and uses an exponential law to model the cumulative fatigue damage.

Li and Kahraman[125,161] proposed a PbM to calculate the fatigue life of point contacts due to micropitting caused by metal–metal contact that was validated with experimental results by assuming crack propagation negligent compared to clack initiation. However, thermal effects were not considered. Li et al.[124] experimentally validated a similar model that predicted wear of point contacts, by integrating the calculation of the friction coefficient and a heat transfer model that estimated the friction coefficient and the temperature. Marble and Morton[119] validated a degradation model for wear caused by spalling in rolling bearings as a function of the area of the defect, the load and material constants. Watson et al.[112] developed an algorithm capable of predicting the RUL of clutches by combining a dynamic model of the system and wear degradation models based on Archard's law presented above taking into account corrosive, adhesive and abrasive wear.

Discussion

In the previous sections, the most common failure modes of gears and bearings of rotating machinery were reviewed with focus on the PHM methods for each failure mode. Special attention was given to the PbM approaches available in the literature. The corresponding degradation mechanisms and PbMs were identified and the potential degradation models presented.

The use of PbMs, particularly for prognostics, has some advantages when compared to DDMs. However, to choose between one or the other, each failure mode has to be analysed independently. As shown in previous sections, many relevant failure modes are not suitable for a PbM approach, because the physics of failure cannot be modelled or because even if the degradation was modelled successfully, the inputs of those models would be unknown. Misalignment, geometrical errors or dirt are common failure modes for which PbMs are particularly challenging.

Another additional difficulty of using PbMs for PHM is the necessary understanding of the physics of failure. If enough data are available, DDM can provide a correlation between the measured variables of a

Downloaded from ade.sagepub.com at Cranfield University on September 22, 2016

system and its health without further analysis of the physics of failure; moreover, if PHM is developed in a variety of systems and failure modes, DDM approaches are scalable, because each system and failure mode does not require a deep analysis of the phenomena as opposed to PbM approaches.

However, large data sets of healthy and faulty conditions are not always available; besides, if new sensors are incorporated, information about their readings would not be available, which means that in many cases additional testing would be needed. An additional aspect, particularly for prognostics, is that DDMs require a significant amount of faulty data sets, but for high valuable assets, for example, aerospace, the failure rate is normally low and faulty data sets are rare.

The necessary understanding of the physics of failure of PbM approaches can be considered as a drawback due to the additional effort and expertise required, but also as an opportunity, because it provides an algorithm based on physical principles in which the relation between the PbM inputs and the health of the system is well understood; thus, the reasoning and health indicators have a physical meaning. A PbM can be modelled with shorter data sets than DDMs, because data are needed for adjusting the parameters and validating the model, whereas DDMs, particularly those based on artificial intelligence, require training data, validation data and are subject to overfitting. In addition, the knowledge about the physics of failure has synergies with the design process and can facilitate the certification, because the principles behind the algorithm are be justified by proven physical principles.

On one hand, DDMs can be used for diagnostics and prognostics, but their architecture is different. For diagnostics, the algorithm should distinguish between two states (healthy and unhealthy), whereas for prognostics the algorithm should identify the degree of degradation and its future heath values, making prognostics particularly challenge for DDMs. On the other hand, PbMs can also be used for diagnostics and prognostics, but for prognostics the assessment of the degree of degradation in the present and future is defined by the degradation model, which is the reason why PbMs are particularly suitable for prognostics. However, the degradation estimated by a PbM differs from the real degradation of the system. If there is an additional way of assessing the degree of degradation, for example, a sensor measuring the temperature of a bearing, directly related to the friction due to metal–metal contact, then a parameter estimator can be used to correct the model parameters and adjust the estimated RUL.

Different degradation models commonly used in rotating machinery have been presented, from simple analytical equations to complex models based on CFD and FEA. All the inputs of a degradation model should be monitored or estimated, which means that when deciding which model should be used, even if a more complex model apparently is more accurate, a simpler model with less inputs and parameters may provide similar results if most of its inputs and parameters must be estimated. The computational time and memory are limited, which can be an additional drawback of using more complex models.

Creep models have been proposed for PHM using the Norton law that relates the deformation as a function of time and temperature. The proposed PbMs have the potential to be used in the future for prognostics of components subject to high temperatures. Fatigue is one of the best known degradation mechanisms. The majority of PbMs for prognostics are based on fatigue principles, either using HCF and LCF models or modelling the crack growth. Therefore, failure modes mainly caused by fatigue are ideal candidates for PbM approaches due to the extensive literature and options available.

In systems subject to mechanical stresses and high temperature, the degradation is caused by fatigue and creep. However, both degradation mechanisms are coupled and cannot be considered independent of each other. The correlation between fatigue and creep is understood and there are PbMs for prognostics in combustor liners and turbine blades, but they are more complex than fatigue or creep models.

Wear is a broad degradation mechanism and the physics behind it differ between dry and lubricated contacts. Dry contacts and fretting are normally modelled using analytical equations but depend on empirical parameters. Prognostics PbMs have been proposed based on wear in dry contacts; however, lubricated contacts are more relevant in rotating machinery.

Wear in lubricated contacts is minimized due to the lubricant film; this film is produced by the relative motion between the surfaces. Under normal condition, wear is negligible, but if the film cannot transmit the load partial metal–metal occurs with the subsequent degradation. The physics of failure are complex because hydrodynamic, mechanical and thermal phenomena are coupled; however, there are several PbMs capable of modelling this degradation mechanism. However, few health condition monitoring algorithms have been proposed.

Conclusion

The area of PbM for health condition monitoring of rotating machinery has been reviewed in this article including the most common parameter estimator techniques and failures modes of rotating machinery along with the models available to represent their degradation mechanisms.

Although comprehensive review papers on PHM for rotating machinery are available, approaches based on PbM have not been extensively reviewed in comparison

Downloaded from ade.sagepub.com at Cranfield University on September 22, 2016

with DDM approaches. The development of a PHM system based on the physics of the system requires a good understanding of the failure modes and their degradation mechanisms. This article aims to serve as a tool to identify common failure modes and their corresponding degradation mechanisms, and to provide a review of the models available to represent the degradation for prognostics based on PbMs.

Rotating machinery components are subject to a variety of failure modes. Although diagnostics for rotating machinery has been extensively studied, research in prognostics is more limited. Vibration analysis and AEs are the main diagnostics and prognostics techniques for gears. PbM approaches commonly consist of a dynamics model of the system that correlates the vibration signal with the stresses plus a crack growth model that estimates the RUL.

In rolling bearings, vibration and AE along with temperature analysis are the most common techniques. PbMs have been applied using a degradation formula similar to Paris law to represent spalling or the identification of the natural frequencies of each rotating component and the amplitude of their response for fault identification and fault isolation. It should also be noted that promising results using AE compared to vibration analysis rely on a high S-N ratio.

Research in PHM for hydrodynamic bearings is more limited. Most of the research focuses on detecting metal–metal contact using temperature, vibration analysis, AEs or metallic particle measurement using DDM approaches. However, the hydrodynamic phenomena are well understood and there are models available, but the potential of these models has not been used for health condition monitoring.

Even if PbMs for PHM have the potential to obtain more accurate predictions, they are not suitable for every system and failure mode. The following limitations of applying PbMs for diagnostics and prognostics should be taken into account:

- Some degradation mechanisms cannot be modelled; thus, PbMs cannot be developed.
- PbM algorithms are not scalable between different systems as opposed to DDM algorithms.
- Expert knowledge is required.
- Additional measurement of the health is preferable to minimize prognosis errors.

However, prognostics PbM approaches have several advantages that can make them ideal for certain systems and failure modes:

- Large data sets are not required as opposed to DDMs.
- Understanding of the system and the physics of failure may be used in other areas (design) and is easily justified for certification purposes.
- Health indicators based on degradation models have a physical meaning.
- The prognostics architecture based on PbMs is defined by the degradation model, whereas prognostics DDMs have complex architectures to identify the current and future degree of degradation.

After this review, it has been shown that relatively simple formulas, for example, creep and fatigue models, can be easily implemented for prognostics based on PbM, while more complex formulas may also be used for more accurate predictions or for complex phenomena where different physics are involved, for example, creep in combination with fatigue or hydrodynamic lubrication combined with metal–metal contact. For more precise results sophisticated models can be used, for example, numerical methods such as FEA or CFD analysis, or models that take into account the microstructure of the material for creep.

It should be noted that a more complex model would led to more accurate predictions assuming that all the parameters required by the model are known. However, the number of sensors is limited and certain parameters can only be estimated; thus, less accurate than if all the parameters are well known. For the design of prognostics capabilities, it may be preferable to develop simple models with measurable parameters instead of complex models that require several assumptions and estimated values. This is due to the following reasons: the accuracy may not be significantly increased if many parameters are estimated, and more complex models require more computational power, which could be a limiting factor in the design of PHM solutions.

Declaration of conflicting interests

The author(s) declared no potential conflicts of interest with respect to the research, authorship and/or publication of this article.

Funding

The author(s) disclosed receipt of the following financial support for the research, authorship and/or publication of this article: The research leading to these results has received funding from the European Union Seventh Framework Programme (FP7/2007-2013) under Grant Agreement No. 605779 (project RepAIR). The text reflects the authors' views. The European Commission is not liable for any use that may be made of the information contained therein. For further information, see http://www.rep-air.eu/. Adrian Uriondo – Proof reading and advice.

Downloaded from ade.sagepub.com at Cranfield University on September 22, 2016

References

1. Kothamasu R, Huang SH and Verduin WH. System health monitoring and prognostics – a review of current paradigms and practices. *Int J Adv Manuf Tech* 2006; 28: 1012–1024.
2. Jennions IK. *Integrated vehicle health management: perspectives on an emerging field*. Warrendale, PA: SAE International, 2011.
3. MacConnell JH. ISHM & design: a review of the benefits of the ideal ISHM system. In: *Proceedings of the 2007 IEEE aerospace conference*, Seattle, WA, 3–10 March 2007, pp.1–18. New York: IEEE.
4. Baroth E, Powers WT, Fox J, et al. IVHM (Integrated Vehicle Health Management) techniques for future space vehicles. In: *Proceedings of the 37th joint propulsion conference and exhibit 2001*, Salt Lake City, UT, 8–11 July 2011, pp.1–10. AIAA.
5. Sikorska JZ, Hodkiewicz M and Ma L. Prognostic modelling options for remaining useful life estimation by industry. *Mech Syst Signal Pr* 2011; 25: 1803–1836.
6. Lee J, Wu F, Zhao W, et al. Prognostics and health management design for rotary machinery systems – reviews, methodology and applications. *Mech Syst Signal Pr* 2014; 42: 314–334.
7. Engel SJ, Gilmartin BJ, Bongort K, et al. Prognostics, the real issues involved with predicting life remaining. In: *Proceedings of the IEEE aerospace conference proceedings*, Big Sky, MT, 18–25 March 2000, vol. 6, pp.457–470. New York: IEEE.
8. Eker OF, Camci F and Jennions IK. Major challenges in prognostics: study on benchmarking prognostics datasets. In: *Proceedings of the PHM*, Dresden, 3–5 July 2012, vol. 3, pp.1–8. PHM Society.
9. Heng A, Zhang S, Tan ACC, et al. Rotating machinery prognostics: state of the art, challenges and opportunities. *Mech Syst Signal Pr* 2009; 23: 724–739.
10. Luo J, Namburu M, Pattipati K, et al. Model-based prognostic techniques [maintenance applications]. In: *Proceedings of the IEEE systems readiness technology conference (AUTOTESTCON 2003)*, Anaheim, CA, 22–25 September 2003, pp.330–340. New York: IEEE.
11. Li C and Liang M. Time–frequency signal analysis for gearbox fault diagnosis using a generalized synchrosqueezing transform. *Mech Syst Signal Pr* 2012; 26: 205–217.
12. Mu-jun X and Shi-Yong X. Fault diagnosis of air compressor based on RBF neural network. In: *Proceedings of the 2011 international conference on mechatronic science, electric engineering and computer (MEC)*, Jilin, China, 19–22 August 2011, pp.887–890. New York: IEEE.
13. Ferreiro S, Arnaiz A, Sierra B, et al. Application of Bayesian networks in prognostics for a new Integrated Vehicle Health Management concept. *Expert Syst Appl* 2012; 39: 6402–6418.
14. Zio E and Di Maio F. Fatigue crack growth estimation by relevance vector machine. *Expert Syst Appl* 2012; 39: 10681–10692.
15. Pantelelis NG, Kanarachos AE and Gotzias N. Neural networks and simple models for the fault diagnosis of naval turbochargers. *Math Comput Simulat* 2000; 51: 387–397.
16. Saxena A and Saad A. Evolving an artificial neural network classifier for condition monitoring of rotating mechanical systems. *Appl Soft Comput* 2007; 7: 441–454.
17. Su H and Chong K-T. Induction machine condition monitoring using neural network modeling. *IEEE T Ind Electron* 2007; 54: 241–249.
18. Reda Taha MM and Lucero J. Damage identification for structural health monitoring using fuzzy pattern recognition (SEMC 2004 structural health monitoring, damage detection and long-term performance; Second international conference on structural engineering, mechanics and computation). *Eng Struct* 2005; 27: 1774–1783.
19. Baraldi P, Mangili F and Zio E. A Kalman filter-based ensemble approach with application to turbine creep prognostics. *IEEE T Reliab* 2012; 61: 966–977.
20. Polikar R. Ensemble based systems in decision making. *IEEE Circ Syst Mag* 2006; 6: 21–45.
21. Jardine AKS, Lin D and Banjevic D. A review on machinery diagnostics and prognostics implementing condition-based maintenance. *Mech Syst Signal Pr* 2006; 20: 1483–1510.
22. Lei Y, Lin J, He Z, et al. A review on empirical mode decomposition in fault diagnosis of rotating machinery. *Mech Syst Signal Pr* 2013; 35: 108–126.
23. Sait AS and Sharaf-Eldeen YI. *A review of gearbox condition monitoring based on vibration analysis techniques diagnostics and prognostics*, vol. 5 (Proceedings of the society for experimental mechanics series). New York: Springer, 2011, pp.307–324.
24. An D, Kim NH and Choi JH. Options for prognostics methods: a review of data-driven and physics-based prognostics. In: *Proceedings of the 54th AIAA/ASME/ASCE/AHS/ASC structures, structural dynamics, and materials conference*, Boston, MA, 8–11 April 2013, pp.1–14. Reston, VA: AIAA.
25. Luo J, Bixby A, Pattipati K, et al. An interacting multiple model approach to model-based prognostics. In: *Proceedings of the 2003 IEEE international conference on systems, man and cybernetics*, Washington, DC, 5–8 October 2003, vol. 1, pp.189–194. New York: IEEE.
26. Li B, Chow M-Y, Tipsuwan Y, et al. Neural-network-based motor rolling bearing fault diagnosis. *IEEE T Ind Electron* 2000; 47: 1060–1069.
27. Paris PC, Gomez MP and Anderson WE. A rational analytic theory of fatigue. *Trend Eng* 1961; 13: 9–14.
28. Corbetta M, Sbarufatti C, Manes A, et al. Sequential Monte Carlo sampling for crack growth prediction providing for several uncertainties. In: *Proceedings of the 2nd European conference of the prognostics and health management society 2014*, Nantes, 8–10 July 2014, vol. 5, pp.1–13. PHM Society.
29. Ray A and Tangirala S. Stochastic modeling of fatigue crack dynamics for on-line failure prognostics. *IEEE T Contr Syst T* 1996; 4: 443–451.
30. Orchard M, Kacprzynski G, Goebel K, et al. Advances in uncertainty representation and management for particle filtering applied to prognostics. In: *Proceedings of the prognostics and health management international*

Downloaded from ade.sagepub.com at Cranfield University on September 22, 2016

conference, Denver, CO, 6–9 October 2008, pp.1–6. New York: IEEE.
31. Oppenheimer CH and Loparo KA. Physically based diagnosis and prognosis of cracked rotor shafts. In: *Proceedings of the components and systems diagnostics, prognostics, and health management II*, Orlando, FL, 1 April 2002, pp.122–132. Bellingham, WA: SPIE.
32. Li CJ and Lee H. Gear fatigue crack prognosis using embedded model, gear dynamic model and fracture mechanics. *Mech Syst Signal Pr* 2005; 19: 836–846.
33. Coppe A, Pais MJ, Kim N-H, et al. Identification of equivalent damage growth parameters for general crack geometry. In: *Proceedings of the annual conference of the prognostics and health management society*, Portland, OR, 10–16 October 2010, pp.1–10. PHM Society.
34. Orsagh RF, Sheldon J and Klenke CJ. Prognostics/diagnostics for gas turbine engine bearings. In: *Proceedings of the 2003 IEEE aerospace conference*, Big Sky, MT, 8–15 March 2003, pp.3095–3103. New York: IEEE.
35. Jaw LC and Wang W. Mathematical formulation of model-based methods for diagnostics and prognostics. In: *Proceedings of the 2006 ASME 51st turbo expo: power for land, sea, and air*, Barcelona, 8–11 May 2006, pp.691–697. New York: ASME.
36. Li Y, Kurfess TR and Liang SY. Stochastic prognostics for rolling element bearings. *Mech Syst Signal Pr* 2000; 14: 747–762.
37. Li Y, Billington S, Zhang C, et al. Adaptive prognostics for rolling element bearing condition. *Mech Syst Signal Pr* 1999; 13: 103–113.
38. Simon D. A comparison of filtering approaches for aircraft engine health estimation. *Aerosp Sci Technol* 2008; 12: 276–284.
39. Wagner J and Shoureshi R. A robust failure diagnostics scheme for nonlinear thermofluid processes. In: *Proceedings of the 1987 American control conference*, Minneapolis, MN, 10–12 June 1987, pp.1877–1882. New York: IEEE.
40. Laroche E, Sedda E and Durieu C. Methodological insights for online estimation of induction motor parameters. *IEEE T Contr Syst T* 2008; 16: 1021–1028.
41. Simani S. Identification and fault diagnosis of a simulated model of an industrial gas turbine. *IEEE T Ind Inform* 2005; 1: 202–216.
42. Peel L. Data driven prognostics using a Kalman filter ensemble of neural network models. In: *Proceedings of the 2008 international conference on prognostics and health management (PHM 2008)*, Denver, CO, 6–9 October 2008, pp.1–6. New York: IEEE.
43. Saha B, Goebel K and Christophersen J. Comparison of prognostic algorithms for estimating remaining useful life of batteries. *T I Meas Control* 2009; 31: 293–308.
44. Baraldi P, Cadinia F, Mangilia F, et al. Prognostics under different available information. *Chem Eng* 2013; 33: 163–168.
45. Tinga T. *Principles of loads and failure mechanisms: applications in maintenance, reliability and design*. London: Springer Science & Business Media, 2013.
46. Castro J and Seabra J. Global and local analysis of gear scuffing tests using a mixed film lubrication model. *Tribol Int* 2008; 41: 244–255.
47. McFadden PD and Toozhy MM. Application of synchronous averaging to vibration monitoring of rolling element bearings. *Mech Syst Signal Pr* 2000; 14: 891–906.
48. Qiu J, Seth BB, Liang SY, et al. Damage mechanics approach for bearing lifetime prognostics. *Mech Syst Signal Pr* 2002; 16: 817–829.
49. Warren AW and Guo YB. Acoustic emission monitoring for rolling contact fatigue of superfinished ground surfaces. *Int J Fatigue* 2007; 29: 603–614.
50. Rahman Z, Ohba H, Yoshioka T, et al. Incipient damage detection and its propagation monitoring of rolling contact fatigue by acoustic emission. *Tribol Int* 2009; 42: 807–815.
51. Hort F, Mazal P and Vlasic F. Monitoring of acoustic emission signal of loaded axial bearings. *J Mater Sci Eng A: Struct Mater Prop Microstruct Process* 2010; 1: 717–724.
52. Hort F and Mazal P. Application of acoustic emission for measuring of contact fatigue of axial bearing. *Eng Mech* 2011; 18: 117–125.
53. Elforjani M and Mba D. Observations and location of acoustic emissions for a naturally degrading rolling element thrust bearing. *J Fail Anal Prev* 2008; 8: 370–385.
54. Guo-Lu L, Zhi-Qiang Z, Hai-Dou W, et al. Acoustic emission monitoring and failure mechanism analysis of rolling contact fatigue for Fe-based alloy coating. *Tribol Int* 2013; 61: 129–137.
55. Sunnersjö CS. Rolling bearing vibrations – the effects of geometrical imperfections and wear. *J Sound Vib* 1985; 98: 455–474.
56. Sawalhi N and Randall RB. Vibration response of spalled rolling element bearings: observations, simulations and signal processing techniques to track the spall size. *Mech Syst Signal Pr* 2011; 25: 846–870.
57. Zhang Z-Q, Li G-L, Wang H-D, et al. Investigation of rolling contact fatigue damage process of the coating by acoustics emission and vibration signals. *Tribol Int* 2012; 47: 25–31.
58. Price ED, Lees AW and Friswell MI. Detection of severe sliding and pitting fatigue wear regimes through the use of broadband acoustic emission. *Proc IMechE, Part J: J Engineering Tribology* 2005; 219: 85–98.
59. Guo YB and Schwach DW. An experimental investigation of white layer on rolling contact fatigue using acoustic emission technique. *Int J Fatigue* 2005; 27: 1051–1061.
60. Tan CK, Irving P and Mba D. A comparative experimental study on the diagnostic and prognostic capabilities of acoustics emission, vibration and spectrometric oil analysis for spur gears. *Mech Syst Signal Pr* 2007; 21: 208–233.
61. Elasha F, Ruiz-Cárcel C, Mba D, et al. Pitting detection in worm gearboxes with vibration analysis. *Eng Fail Anal* 2014; 42: 366–376.
62. Feng Z and Liang M. Fault diagnosis of wind turbine planetary gearbox under nonstationary conditions via adaptive optimal kernel time–frequency analysis. *Renew Energ* 2014; 66: 468–477.
63. Tan CK and Mba D. Identification of the acoustic emission source during a comparative study on diagnosis of a spur gearbox. *Tribol Int* 2005; 38: 469–480.

Downloaded from ade.sagepub.com at Cranfield University on September 22, 2016

64. Peng Z and Kessissoglou N. An integrated approach to fault diagnosis of machinery using wear debris and vibration analysis. *Wear* 2003; 255: 1221–1232.
65. Kim Y-H, Tan ACC, Mathew J, et al. Condition monitoring of low speed bearings: a comparative study of the ultrasound technique versus vibration measurements. In: *Proceedings of the 1st world congress on engineering asset management (WCEAM)*, Gold Coast, QLD, Australia, 11–14 July 2006, pp.182–191. London: Springer.
66. Choudhury A and Tandon N. Application of acoustic emission technique for the detection of defects in rolling element bearings. *Tribol Int* 2000; 33: 39–45.
67. He Y, Zhang X and Friswell MI. Observation of time-frequency characteristics of the acoustic emission from defects in rolling element bearings. *Insight* 2010; 52: 412–418.
68. Jamaludin N and Mba D. Monitoring extremely slow rolling element bearings: part I. *NDT&E Int* 2002; 35: 349–358.
69. Jamaludin N and Mba D. Monitoring extremely slow rolling element bearings: part II. *NDT&E Int* 2002; 35: 359–366.
70. Zakrajsek JJ and Lewicki DG. Detecting gear tooth fatigue cracks in advance of complete fracture. *Tribotest* 1998; 4: 407–422.
71. Ha JM, Park J, Youn BD, et al. Fault diagnostics of planet gears in wind turbine using autocorrelation-based time synchronous averaging (ATSA). In: *Proceedings of the second European conference of the prognostics and health management society 2014*, Nantes, 8–10 July 2014, pp.1–8. PHM Society.
72. Sun J, Wood RJK, Wang L, et al. Wear monitoring of bearing steel using electrostatic and acoustic emission techniques. *Wear* 2005; 259: 1482–1489.
73. Harvey TJ, Wood RJK and Powrie HEG. Electrostatic wear monitoring of rolling element bearings. *Wear* 2007; 263: 1492–1501.
74. Boness RJ and McBride SL. Adhesive and abrasive wear studies using acoustic emission techniques. *Wear* 1991; 149: 41–53.
75. Feng Z, Zuo MJ, Hao R, et al. Gear crack assessment based on cyclic correlation analysis. In: *Proceedings of the 8th international conference on reliability, maintainability and safety (ICRMS 2009)*, Chengdu, China, 20–24 July 2009, pp.1071–1076. New York: IEEE.
76. Kacprzynski GJ, Roemer GJ, Modgil G, et al. Enhancement of physics-of-failure prognostic models with system level features. In: *Proceedings of the 2002 IEEE aerospace conference*, Big Sky, MT, 9–16 March 2002, vol. 6, pp.2919–2925. New York: IEEE.
77. Kacprzynski GJ, Sarlashkar A, Roemer MJ, et al. Predicting remaining life by fusing the physics of failure modeling with diagnostics. *JOM: J Min Met Mat S* 2004; 56: 29–35.
78. Paya BA, Esat II and Badi MNM. Artificial neural network based fault diagnostics of rotating machinery using wavelet transforms as a preprocessor. *Mech Syst Signal Pr* 1997; 11: 751–765.
79. Tang B, Song T, Li F, et al. Fault diagnosis for a wind turbine transmission system based on manifold learning and Shannon wavelet support vector machine. *Renew Energ* 2014; 62: 1–9.
80. Jack LB and Nandi AK. Fault detection using support vector machines and artificial neural networks, augmented by genetic algorithms. *Mech Syst Signal Pr* 2002; 16: 373–390.
81. Du Y, Zhang W, Zhang Y, et al. Fault diagnosis of rotating machines for rail vehicles based on local mean decomposition – energy moment – directed acyclic graph support vector machine. *Adv Mech Eng* 2016; 8: 1–6.
82. Sun X, Tan J, Wen Y, et al. Rolling bearing fault diagnosis method based on data-driven random fuzzy evidence acquisition and Dempster–Shafer evidence theory. *Adv Mech Eng* 2016; 8: 1–8.
83. Wu TY, Chen JC and Wang CC. Characterization of gear faults in variable rotating speed using Hilbert-Huang Transform and instantaneous dimensionless frequency normalization. *Mech Syst Signal Pr* 2012; 30: 103–122.
84. Maru MM, Castillo RS and Padovese LR. Study of solid contamination in ball bearings through vibration and wear analyses. *Tribol Int* 2007; 40: 433–440.
85. Okamoto K, Shiihara H, Nagayama Y, et al. Effective condition monitoring methods for diesel main bearing: high frequency vibration measurement and wear particle detection. *Jpn Inst Mar Eng* 2007; 42: 560–565.
86. Moosavian A, Ahmadi H, Tabatabaeefar A, et al. Comparison of two classifiers; K-nearest neighbor and artificial neural network, for fault diagnosis on a main engine journal-bearing. *Shock Vib* 2013; 20: 263–272.
87. British Standard BS 7848:1996 (ISO 10825:1995). GEARS – wear and damage to gear teeth – terminology.
88. Ding Y and Rieger NF. Spalling formation mechanism for gears. *Wear* 2003; 254: 1307–1317.
89. The Barden Corporation. *Bearing failure: causes and cures*. Schaeffler, Barden Precis Bear, 2007.
90. SKF Group. SKF lubrication management, 2011, http://www.skf.com/binary/12-107550/12114-EN_SKFLubrication-Management.pdf
91. Iyer NS, Hai Q, Weizhong Y, et al. Early detection of lubrication anomalies in oil-lubricated bearings. In: *Proceedings of the 2007 ASME turbo expo: power for land, sea, and air*, Montreal, QC, Canada, 14–17 May 2007, pp.785–794. New York: ASME.
92. El-Thalji I and Jantunen E. A summary of fault modelling and predictive health monitoring of rolling element bearings. *Mech Syst Signal Pr* 2005; 60–61: 252–272.
93. Howard I. *A review of rolling element bearing vibration detection, diagnosis and prognosis* (AR-008-399). Department of Defence, Defence Science and Technology Organization, 1994.
94. Tandon N and Choudhury A. A review of vibration and acoustic measurement methods for the detection of defects in rolling element bearings. *Tribol Int* 1999; 32: 469–480.
95. Halme J and Andersson P. Rolling contact fatigue and wear fundamentals for rolling bearing diagnostics – state of the art. *Proc IMechE, Part J: J Engineering Tribology* 2009; 224: 377–393.
96. Randall RB and Antoni J. Rolling element bearing diagnostics – a tutorial. *Mech Syst Signal Pr* 2011; 25: 485–520.

Downloaded from ade.sagepub.com at Cranfield University on September 22, 2016

97. Zong H, Wang H and Hong R. Dynamic research on single-row slewing bearing with local spalling of inner ring. *Adv Mech Eng* 2016; 8: 1–10.
98. *Clevite 77 engine bearing failure and analysis guide*. Form # CL77-3-402. Dana Corporation, https://www.scribd.com/document/101902715/Engine-bearing-failure-analysis-guide
99. Zeidan FY and Herbage BS. Fluid film bearing fundamentals and failure analysis. In: *Proceedings of the 20th turbomachinery symposium*, Texas A&M University, College Station, TX, 1991, pp.161–186.
100. Wang Q. Seizure failure of journal-bearing conformal contacts. *Wear* 1997; 210: 8–16.
101. Tanaka M. Journal bearing performance under starved lubrication. *Tribol Int* 2000; 33: 259–264.
102. Huang Q, Wang J, Ma L, et al. Fatigue damage mechanism of oil film bearing sleeve. *J Iron Steel Res Int* 2007; 14: 60–68.
103. Vencl A and Rac A. Diesel engine crankshaft journal bearings failures: case study. *Eng Fail Anal* 2014; 44: 217–228.
104. Mirhadizadeh SA and Mba D. Observations of acoustic emission in a hydrodynamic bearing. *J Qual Mainten Eng* 2008; 15: 193–201.
105. Chin HH. Turbine engine hot section prognostics. In: *Proceedings of the 59th meeting of the society for machinery failure prevention technology: essential technologies for successful prognostics*, Virginia Beach, VA, 18–21 April 2005, pp.45–53. MFPT Society.
106. Yu Q and Zhou H. Study on creep damage and life prediction of threaded connections at high temperature. *Adv Mech Eng* 2016; 8: 1–9.
107. Vogel WH, Soderquist RW and Schlein BC. Prediction of crack initiation in combustion chamber liners. *J Aircraft* 1977; 14: 1076–1080.
108. Daroogheh N, Vatani A, Gholamhossein M, et al. Engine life evaluation based on a probabilistic approach. In: *Proceedings of the ASME 2012 international mechanical engineering congress and exposition (IMECE)*, Houston, TX, 9–15 November 2012, pp.347–358. New York: ASME.
109. Bray DP, Dennis RJ and Bradford RAW. Modelling the complex manufacturing history of a pipework joint and assessment of its through life creep-fatigue damage using finite element based methods. In: *Proceedings of the ASME 2010 pressure vessels and piping division/K-PVP conference*, Bellevue, WA, 18–22 July 2010, pp.401–419. New York: ASME.
110. Wu X, Yandt S and Zhang Z. A framework of integrated creep-fatigue modeling. In: *Proceedings of the ASME turbo expo 2009: power for land, sea, and air*, Orlando, FL, 8–12 June 2009, pp.731–736. New York: ASME.
111. Tinga T, Brekelmans WAM and Geers MGD. Time-incremental creep–fatigue damage rule for single crystal Ni-base superalloys. *Mat Sci Eng A: Struct* 2009; 508: 200–208.
112. Watson M, Byington C, Edwards D, et al. Dynamic modeling and wear-based remaining useful life prediction of high power clutch systems. *Tribol T* 2005; 48: 208–217.
113. Fu S and Gao Y. Fan blade crack diagnosis method study. *Adv Mech Eng* 2016; 8: 1–8.
114. Pais MJ and Kim NH. Predicting fatigue crack growth under variable amplitude loadings with usage monitoring data. *Adv Mech Eng* 2015; 7: 1–11.
115. Walvekar AA, Leonard BD, Sadeghi F, et al. An experimental study and fatigue damage model for fretting fatigue. *Tribol Int* 2014; 79: 183–196.
116. Leonard BD, Patil P, Slack TS, et al. Fretting wear modeling of coated and uncoated surfaces using the combined finite-discrete element method. *J Tribol: T ASME* 2011; 133: 021601-1–021601-12.
117. Kasarekar AT, Sadeghi F and Tseregounis S. Fretting fatigue of rough surfaces. *Wear* 2008; 264: 719–730.
118. Quraishi SM, Khonsari MM and Baek DK. A thermodynamic approach for predicting fretting fatigue life. *Tribol Lett* 2005; 19: 169–175.
119. Marble S and Morton BP. Predicting the remaining life of propulsion system bearings. In: *Proceedings of the 2006 IEEE aerospace conference proceedings*, Big Sky, MT, 4–11 March 2006, pp.1–8. New York: IEEE.
120. Slack T and Sadeghi F. Explicit finite element modeling of subsurface initiated spalling in rolling contacts. *Tribol Int* 2010; 43: 1693–1702.
121. Hoeprich MR. Rolling element bearing fatigue damage propagation. *J Tribol: T ASME* 1992; 114: 328–333.
122. Li Y, Billington S, Zhang C, et al. Dynamic prognostic prediction of defect propagation on rolling element bearings. *Tribol T* 1999; 42: 385–392.
123. Kotzalas MN and Harris TA. Fatigue failure progression in ball bearings. *J Tribol: T ASME* 2000; 123: 238–242.
124. Li S, Kahraman A, Anderson N, et al. A model to predict scuffing failures of a ball-on-disk contact. *Tribol Int* 2013; 60: 233–245.
125. Li S and Kahraman A. A fatigue model for contacts under mixed elastohydrodynamic lubrication condition. *Int J Fatigue* 2011; 33: 427–436.
126. Singh MP, Thakur BK and Sullivan WE. Assessing useful life of turbomachinery components. In: *Proceedings of the 34th turbomachinery symposium*, Texas A&M University, College Station, TX, September 2005, pp.177–192.
127. Tinga T, Brekelmans WAM and Geers MGD. Incorporating strain gradient effects in a multiscale constitutive framework for nickel-base superalloys. *Philos Mag* 2008; 88: 3793–3825.
128. Tinga T, Brekelmans WAM and Geers MGD. Cube slip and non-Schmid effects in single crystal Ni-base superalloys. *Model Simul Mater Sc* 2009; 18: 015005.
129. Rabotnov Y. Creep problems in structural members. *North-Holland Ser Appl Math Mech* 1971; 51: 575–576.
130. Kachanov LM. *Introduction to continuum damage mechanics*. Dordrecht: Springer, 1986.
131. Wöhler A. Versuche über die Festigkeit der Eisenbahnwagenachsen. *Z Bauwes* 1860; 10: 160–161.
132. British Standard. *Guide to fatigue design and assessment of steel products*. London: BSI Standards Publication, 2014.
133. Basquin OH. The exponential law of endurance tests. *Am Soc Test Mater* 1910; 10: 625–630.

Downloaded from ade.sagepub.com at Cranfield University on September 22, 2016

134. Boardman B. Fatigue resistance of steels. In: *ASM international metals handbook*, vol. 1. 10th ed. Materials Park, OH: ASM International, 1990, pp.673–688.
135. Manson S and Coffin LF. *Behavior of materials under conditions of thermal stress*. Report no. NACA TN 2933, 1954. Cleveland, OH: National Advisory Committee for Aeronautics.
136. Coffin L. Apparatus for study of effects of cyclic thermal stresses on ductile metals. *Trans ASME* 1954; 76: 931–950.
137. Miner MA. Cumulative damage in fatigue. *J Appl Mech* 1945; 12: 159–164.
138. Sadeghi F, Jalalahmadi B, Slack TS, et al. A review of rolling contact fatigue. *J Tribol: T ASME* 2009; 131: 1–15.
139. Manson SS, Halford GR and Spera DA. *The role of creep in high temperature low cycle fatigue*. Advances in creep design, no. A72-37701, 1 January 1971. New York: Halstead Press, pp.229–249.
140. Amiri M and Khonsari MM. On the thermodynamics of friction and wear – a review. *Entropy* 2010; 12: 1021–1049.
141. Dasgupta A and Pecht M. Material failure mechanisms and damage models. *IEEE T Reliab* 1991; 40: 531–536.
142. Ghosh A, Paulson N and Sadeghi F. A fracture mechanics approach to simulate sub-surface initiated fretting wear. *Int J Solids Struct* 2015; 58: 335–352.
143. Coulomb CA. *Theorie des Machines Simples: en Ayant egard au frottement de leurs parties et a la roideur des cordages*. Paris: Mémories de Mathématique et de Physique de l'Académie Royale des Sciences: X, 1785, pp.161–342.
144. Reynolds O. On the theory of lubrication and its application to Mr. Beauchamp tower's experiments, including an experimental determination of the viscosity of olive oil. *Philos T R Soc Lond* 1886; 40: 191–203.
145. Stachowiak GW and Batchelor AW. *Engineering tribology*. 4th ed. Burlington, MA: Elsevier, 2013.
146. Sinanoglu C, Kurban AO and Yildirim S. Analysis of pressure variations on journal bearing system using artificial neural network. *Ind Lubr Tribol* 2004; 56: 74–87.
147. Choi J, Kim SS, Rhim SS, et al. Numerical modeling of journal bearing considering both elastohydrodynamic lubrication and multi-flexible-body dynamics. *Int J Automot Techn* 2012; 13: 255–261.
148. Stefani F and Rebora A. Steadily loaded journal bearings: quasi-3D mass–energy-conserving analysis. *Tribol Int* 2009; 42: 448–460.
149. Jin H and Zuo W. Simulation and heat transfer calculation on a journal bearing with a center circumferential groove in load zone. *Int J Adv Comput Technol* 2013; 5: 54–61.
150. Gelinck ERM and Schipper DJ. Calculation of Stribeck curves for line contacts. *Tribol Int* 2000; 33: 175–181.
151. Liu Q. *Friction in mixed and elastohydrodynamic lubricated contacts including thermal effects*. PhD Thesis, University of Twente, Enschede, 2002.
152. Lu X, Khonsari MM and Gelinck ERM. The Stribeck curve: experimental results and theoretical prediction. *J Tribol: T ASME* 2006; 128: 789–794.
153. Greenwood JA and Williamson JBP. Contact of nominally flat surfaces. *P Roy Soc A: Math Phy* 1966; 295: 300–319.
154. Faraon IC. *Mixed lubrication of line contacts*. PhD Thesis, University of Twente, Enschede, 2005.
155. Faraon IC and Schipper DJ. Stribeck curve for starved line contacts. *J Tribol: T ASME* 2007; 129: 181–187.
156. Hua DY, Qiu L and Cheng HS. Modeling of lubrication in micro contact. *Tribol Lett* 1997; 3: 81–86.
157. Hu Y-Z and Zhu D. A full numerical solution to the mixed lubrication in point contacts. *J Tribol: T ASME* 2000; 122: 1–9.
158. Wang Y, Zhang C, Wang QJ, et al. A mixed-TEHD analysis and experiment of journal bearings under severe operating conditions. *Tribol Int* 2002; 35: 395–407.
159. Wang Y, Lin F, Jiang H, et al. Investigation on frictional characteristic of deep-groove ball bearings subjected to radial loads. *Adv Mech Eng* 2015; 7: 1–12.
160. Zhang C, Cheng HS and Wang QJ. Scuffing behavior of piston-pin/bore bearing in mixed lubrication – part II: scuffing mechanism and failure criterion. *Tribol T* 2004; 47: 149–156.
161. Li S and Kahraman A. A physics-based model to predict micro-pitting lives of lubricated point contacts. *Int J Fatigue* 2013; 47: 205–215.

Downloaded from ade.sagepub.com at Cranfield University on September 22, 2016



https://dspace.org/

A review of physics-based models in prognostics: application to gears and bearings of rotating machinery

Cubillo, Adrian; Perinpanayagam, Suresh; Esperon Miguez, Manuel

2016-08-26

Hindawi Publishing Corporation / SAGE Publications

https://dspace.lib.cranfield.ac.uk/handle/1826/10597

Cubillo A, Perinpanayagam S, Esperon-Miguez M, A review of physics-based models in prognostics: application to gears and bearings of rotating machinery Advances in Mechanical Engineering, 2016, Vol. 8(8), pp 1–21

Downloaded from a DSpace repository. https://dspace.org/